Stress and its effect on optical properties of AlN nanorods

X. H. Ji,[1] Q. Y. Zhang,[1,a)] Z. Y. Ling,[1] and S. P. Lau[2,b)]
[1]*MOE Key Laboratory of Specially Functional Materials, South China University of Technology, Guangzhou 510641, People's Republic of China*
[2]*Department of Applied Physics, The Hong Kong Polytechnic University, Hung Hom, Kowloon, Hong Kong*

(Received 18 October 2009; accepted 14 November 2009; published online 7 December 2009)

The stress states in AlN nanorods deposited on Si and its effect on optical properties have been investigated by means of Raman scattering and photoluminescence methods. The observed frequency downshift and linewidth broadening from temperature-dependent Raman scattering can be well described by an empirical relationship taking into account the contributions of the thermal expansion and decay of optical phonons. The phonon-energy difference of the E_2(high) mode between the stress-free bulk-AlN and AlN nanorods appears to increase with increasing temperature, demonstrating that differential thermal expansion between the Si-substrate and AlN nanorods is the key parameter reflecting the stress in the nanorods. © *2009 American Institute of Physics*. [doi:10.1063/1.3271774]

As building blocks for future nanodevices and an ideal platform for the fundamental physical research in nanoscale, one-dimensional semiconductor nanostructures have currently become a focus of intense research.[1–4] Aluminum nitride (AlN), one of the wide bandgap semiconductors, is highly attractive because of its outstanding thermal conductivity and stability, high electrical resistivity, hardness, high resistance to chemicals, and high melting point.[5–7] In particular, several potential applications using AlN nanostructures have been proposed including gas sensors, field emission device, and nanoscale light-emitting diodes.[8–11] In the growth of nanomaterials, an appropriate substrate is essential to obtain high-quality well-aligned nanostructures. Silicon (Si), has both good electrical and thermal conductivity, and enable to integration of devices with Si-based electronics, is considered as one of the most suitable substrates for nitrides. However, the lattice mismatch between Si and AlN will induce stress. Acquisition knowledge of strain or stress state in AlN nanorods is significantly important toward better understanding AlN nanorods properties and fabricating the nanorods-based electronic and optoelectronic devices with a desired performance.

Herein, the stress suffered in the AlN nanorods has been studied in detail by means of Raman scattering. It is found that tensile stress exists in the AlN nanorods deposited on Si is comparable to that of AlN nanowires on sapphire[12] although the lattice mismatch is much larger on Si. The stress is mainly induced by differential thermal expansion between the Si substrate and AlN nanorods.

AlN nanorods were prepared in a horizontal tube furnace. The experimental details have been reported elsewhere.[13] In brief, aluminum chloride powder ($AlCl_3$, Sigma-Aldrich, 99.99%) and ammonium (NH_3) were used as aluminum and nitrogen sources, respectively. AlN nanorods were grown on Si (100) substrate without catalyst at 1000 °C for about 2 h. Crystallography of the AlN nanorods was determined by using x-ray diffractometer (XRD) (Siemens D5005). Field emission scanning electron microscope (JEOL JSM-6340F) and transmission electron microscope (TEM) (JEOL JEM-2010) were used for the nanostructural morphologies and crystal structure analysis. The Raman spectra were taken with a Renishaw micro-Raman spectrometer in back-scattering geometry, equipped with 514 nm Ar^+ laser as the excitation source and focused on the sample through a long working distance 50× objective. A Linkham temperature stage with a quartz window was used to vary the sample temperature from 77 to 480 K in flowing liquid nitrogen during the Raman measurements. For each measurement point, the temperature was stabilized for ten minutes before acquiring a spectrum. Photoluminescence (PL) measurements were carried out by using a 266 nm frequency-quadruple Nd:YAG pulsed laser.

Typical SEM images of the as-grown samples are shown in Figs. 1(a) and 1(b). Figure 1(a) is the tilted-view image revealing that entire substrate was covered with uniform and well-aligned AlN nanorods. The nanorods are in obvious hexagon shape as shown in plain-view image in Fig. 1(b). Typical diameter and length of the AlN nanorods is around

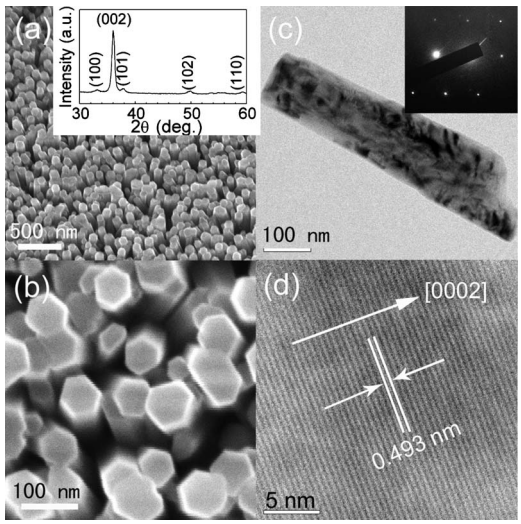

FIG. 1. [(a) and (b)] The tilted-view and plain-view SEM images of the AlN nanorods on Si substrates, the inset is the typical XRD pattern of the AlN nanorod arrays. (c) TEM image of a single AlN nanorod, the inset is the corresponding SAED pattern. (d) HRTEM image of the AlN nanorod.

a)Electronic mail: qyzhang@scut.edu.cn.
b)Electronic mail: apsplau@polyu.edu.hk.

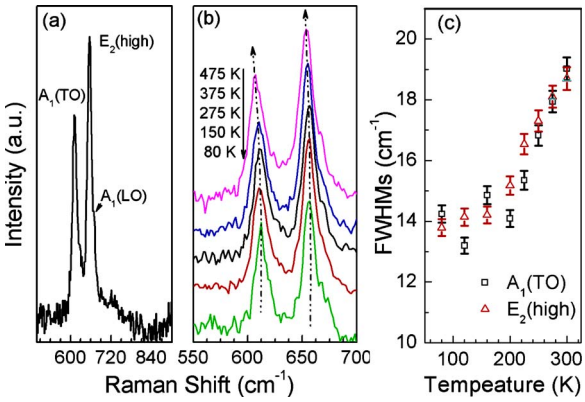

FIG. 2. (Color online) (a) Raman spectrum of the AlN nanorods at RT. (b) Raman spectra of the AlN nanorods at selected temperatures. (c) FMWHs of A_1(TO) and E_2(high) modes in dependence on the temperature.

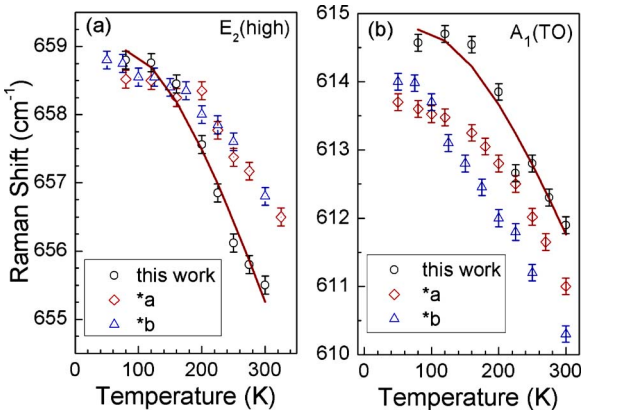

FIG. 3. (Color online) Raman shift of A_1(TO) and E_2(high) modes of the AlN nanorods as a function of temperature, data of a* and b* were taken from Refs. 15 and 16, respectively. The solid lines are fitting curves using Eq. (2).

50–80 nm and ~1 μm, respectively. It is noted that the AlN are quasialigned normal to the Si substrate and approximately in the same height. The inset of Fig. 1(a) displays XRD pattern of the AlN nanorod arrays on Si substrates, exhibiting typical AlN wurtzite structure. Miller indices are indicated on each diffracted peak. There are no characteristic peaks of impurities like metal Al, oxide, or other compounds within the resolution. The intense hexagonal AlN (0002) peak indicates that the AlN crystals grow preferentially along c-axis. The structural characterization of a single AlN was carried out by TEM as shown in Figs. 1(c) and 1(d). The inset of Fig. 1(c) is the corresponding selected-area electron diffraction (SAED) pattern. Figure 1(d) presents the high-resolution TEM (HRTEM) image of the AlN nanorod, showing clear and perfect lattice fringes. The lattice spacing of 0.493 nm in the growth direction corresponds to the (0001) plane of wurtzite AlN. Both the SAED pattern and the HR-TEM image confirm the result of XRD analysis that the AlN nanorods in wurtzite structure preferentially grow along the c-axis direction.

Figure 2(a) shows a typical Raman spectrum of the as-prepared AlN nanorods at room temperature (RT). Two fingerprint phonons of hexagonal AlN, A_1(TO) and E_2(high), are obviously observed at RT, which are centered at 612 and 655.5 cm^{-1}, respectively. The peak positions and the full-width at half-maximums (FWHMs), however, differ from the characteristic frequencies of the unstrained AlN reported.[14–16] The Raman shift of E_2(high) mode indicates the presence of internal stress and the line broadening of the E_2(high) mode indicates the existence of the defects.[14] Compressive and tensile stress of the sample will shift the peak to a higher and a lower wavenumber. It has been used to estimate the magnitude of the stress between the AlN and substrate. In the linear approximation, the deviation in frequency of a given phonon mode γ under symmetry-conserving stress can be expressed in terms of the biaxial stress σ_{xx} (Refs. 12 and 17)

$$\Delta\omega_\gamma = K_\gamma \sigma_{xx}, \tag{1}$$

where K_γ is the linear stress coefficient, and was taken as 3.39 cm^{-1}/GPa. In our case, Raman shift of each active mode was determined using the mixed Gaussian and Lorentzian line shape fitting. The redshift of the E_2(high) mode corresponding to 657 cm^{-1} (Refs. 15 and 16) of the fitted value of 655.5 cm^{-1} demonstrated that AlN nanorods grown on the Si substrate are under tensile stress, which was estimated to be 0.44 GPa. FWHMs of A_1(TO) and E_2(high) modes as a function of temperature are shown in the Fig. 2(c). The FWHMs is ~10 cm^{-1} larger than the bulk AlN. It is well known that the FWHM in Raman spectra is inversely proportional to the phonon lifetime because the reduced dimensions of nanomaterials lead to the confined phonons to scatter severely and to relax at the interface. Furthermore, the Raman linewidth were found to be affected by impurities or defects in semiconductors, which in turn lead to the shortening of the phonon lifetime. Therefore, both phonon boundary relaxation and the additional channel of phonon scattering at impurity or defect centers contribute to the broadening in Raman linewidth.

We further investigated temperature-dependent Raman scattering of AlN nanorods deposited on Si substrate. Figure 2(b) displays the selected Raman spectra of AlN nanorods obtained at five different temperatures. The changes in the Raman line position, FWHMs, and in intensity are clearly evident. The Raman line position of the A_1(TO) and E_2(high) modes as a function of temperature in the range of 80–300 K are shown in Figs. 3(a) and 3(b), respectively. For comparison, the measured temperature-dependent optical frequency shift in the Raman spectrum of the A_1(TO) and the E_2 modes for bulk (stress-free) AlN reproduced from Refs. 15 and 16 are displayed in the figures. The effects of temperature on the phonon energy measured by Raman scattering are primarily due to the thermal expansion of the lattice, a downshift of phonon frequency with temperature is expected. An improved empirical formula [Eq. (2)] has been used by Hayes *et al.*[16] for bulk AlN.

$$\omega(T) = \omega_0 - \frac{A}{e^{B(hc\omega_0/k_BT)} - 1}, \tag{2}$$

where ω_0 is the Raman photon frequency at 0 K, ω_0, A and B are fitting parameters. The solid lines in Figs. 3(a) and 3(b) indicate that the empirical equation fits well with experiment data for both A_1(TO) and E_2(high) modes. The fitting parameters ω_0, A and B are ~614.9±0.4, 6.4±3.8 and 0.32±0.14 cm^{-1} for A_1(TO), and ~658.7±0.4, 3.9±2.8 and 0.25±0.15 cm^{-1} for E_2(high), respectively. The fitting frequencies at 0 K of both modes are close to those of reported bulk AlN. It is clear that the phonon frequency of the E_2 mode is higher for stress-free AlN than that of AlN nano-

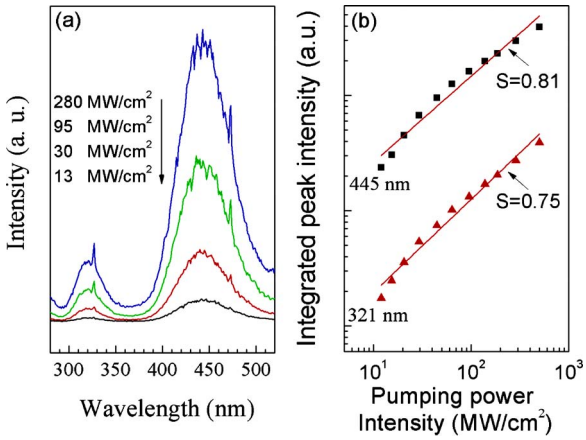

FIG. 4. (Color online) (a) PL spectra from the AlN nanorods upon selected excitation power. (b) PL peak intensity as a function of the laser power. The solid lines in the figures are linear fitted.

rods on Si substrate. But for the A_1(TO) mode, the behavior is reversed. The confinement is anisotropic which has different effect on different phonon modes, and as a result the Raman shift of each mode is different. It is noteworthy that the phonon energy difference of the E_2 mode between the stress-free AlN and AlN nanorods on Si appears to increase with increasing temperature as shown in Fig. 3(a). This suggests that differential thermal expansion between the Si substrate and AlN nanorods is the key contribution to the tensile stress in the nanorods, and the lower the temperature, the less the Si substrate effects on the AlN nanorods phonons.

Figure 4(a) shows the PL emission from AlN nanorods. Intense UV emission around 321 nm (3.87 eV), and visible emission of 445 nm (2.8 eV), have clearly been observed. It has been established that the luminescence intensity I can be expressed as[18]

$$I = \eta I_0^{\alpha}, \tag{3}$$

where I_o is the power of the excitation laser, η is the emission efficiency, and the exponent α represents the radiative recombination mechanism. For excitonic recombination, $1 < \alpha < 2$; for band-gap emission, $\alpha \approx 2$; α is less than 1 when an impurity is involved in the transition as well as for donor-acceptor transition.[18] We found that the PL characteristics of AlN nanorods can be analyzed via Eq. (3). Figure 4(b) represents the PL intensity as a function of the excitation laser power in logarithm scale of AlN nanorods at RT. Linear fitting of the data revealed the slopes of the line are less than one, suggesting that the emission getting saturated in high excitation power. Large surface to volume ratio of the AlN nanorods, efficient and fast trapping of photogenerated holes at surface sites can be expected.[19] In the case of subbandgap excitation, only bands related to the transitions between levels situated in the bandgap could be observed. Intrinsic defects such as interstitial Al ions or nitrogen vacancies as well as oxygen-related defects were assumed to be the recombination centers. In this case, the UV emission is attributed to oxygen related defect complexes, when oxygen substitutes for nitrogen in the AlN lattice. It shifts from 3.3 to 4.0 eV with the oxygen concentration as reported.[20] The nitrogen vacancy and Al interstitial point defects are responsible for the visible emission as suggested by Strassburg *et al.*[21] Unlike the extremely broadband emission from AlN,[22,23] the FWHM of the emissions of AlN nanorods is about 15 and 70 nm, corresponding to UV and visible emission, respectively. The PL measurement provides strong evidence for the existence of a shortening phonon lifetime mechanism via impurities and defects.

In conclusion, the AlN nanorods exhibited tensile stress of 0.44 GPa which was estimated from the E_2(high) phonon shift. The frequencies of the A_1(TO) and E_2(high) modes downshifted and the linewidths broadened as temperature increasing, which results from the thermal expansion difference between Si and AlN. The result of the excitation power dependent PL confirms that the defects lead to shortening in the phonon lifetime.

This work is supported by SRF for ROCS, SEM (Grant No. [2008]890) and Natural Science Foundation of Guangdong Province (Grant No. 9451064101002440).

[1] Y. Cui and C. M. Lieber, Science **291**, 851 (2001).
[2] Z. W. Pan, Z. R. Dai, and Z. L. Wang, Science **291**, 1947 (2001).
[3] X. F. Duan, Y. Huang, R. Agrwal, and C. M. Lieber, Nature (London) **421**, 241 (2003).
[4] C. Q. Sun, Prog. Mater. Sci. **54**, 179 (2009).
[5] F. Davis, Proc. IEEE **79**, 702 (1991).
[6] J. H. Edgar, S. Strite, I. Akasaki, H. Amano, and C. Metzel, *Properties, Processing, and Applications of Gallium Nitride and Related Semiconductors, Part A* (INSPEC, London, 1999).
[7] J. Li, Z. Y. Fan, R. Dahal, M. L. Nakarmi, J. Y. Lin, and H. X. Jiang, Appl. Phys. Lett. **89**, 213510 (2006).
[8] Y. B. Tang, H. T. Cong, and H. M. Cheng, NANO **2**, 307 (2007).
[9] Q. Wang, Q. Sun, P. Jena, and Y. Kawazoe, ACS Nano **3**, 621 (2009).
[10] Z. Zhou, J. J. Zhao, Y. S. Chen, P. V. Schleyer, and Z. F. Chen, Nanotechnology **18**, 424023 (2007).
[11] J. Zheng, Y. Yang, B. Yu, X. Song, and X. Li, ACS Nano **2**, 134 (2008).
[12] Q. Zhao, H. Zhang, X. Xu, Z. Wang, J. Xu, D. Yu, G. Li, and F. Su, Appl. Phys. Lett. **86**, 193101 (2005).
[13] X. H. Ji, S. P. Lau, S. F. Yu, H. Y. Yang, T. S. Herng, and J. S. Chen, Nanotechnology **18**, 105601 (2007).
[14] M. Kuball, F. Demangeot, J. Frandon, M. A. Renucci, N. Grandjean, and O. Briot, MRS Internet J. Nitride Semicond. Res. **4S1**, G6.28 (1999).
[15] M. Kazan, Ch. Zgheib, E. Moussaed, and P. Masri, Diamond Relat. Mater. **15**, 1169 (2006).
[16] J. M. Hayes, M. Kuball, Y. Shi, and J. H. Edgar, Jpn. J. Appl. Phys., Part 2 **39**, L710 (2000).
[17] D. G. Zhao, S. J. Xu, M. H. Xie, S. Y. Tong, and H. Yang, Appl. Phys. Lett. **83**, 677 (2003).
[18] L. Bergman, X.-B. Chen, J. L. Morrison, J. Huso, and A. P. Purdy, J. Appl. Phys. **96**, 675 (2004).
[19] A. van Dijken, E. A. Meulenkamp, D. Vanmaekelbergh, and A. Meijerink, J. Phys. Chem. B **104**, 1715 (2000).
[20] A. Sarua, S. Rajasingam, M. Kuball, N. Garro, O. Sancho, A. Cros, A. Cantarero, D. Olguin, B. Liu, D. Zhuang, and J. H. Edgar, Mater. Res. Soc. Symp. Proc. **798**, Y5.17 (2004).
[21] M. Strassburg, J. Senawiratne, N. Dietz, U. Haboeck, A. Hoffmann, V. Noveski, R. Dalmau, R. Schlesser, and Z. Sitar, J. Appl. Phys. **96**, 5870 (2004).
[22] S. Pacesove and L. Jastrabik, J. Phys. B **29**, 913 (1979).
[23] C. Xu, L. Xue, C. Yin, and G. Wang, Phys. Status Solidi A **198**, 329 (2003).